ARCHIVES
of
FOUNDRY ENGINEERING

ISSN (2299-2944)
Volume 2026
Issue 3/2026

5 – 10

1/3

10.24425/afe.2026.158012

Published quarterly as the organ of the Foundry Commission of the Polish Academy of Sciences

Microstructure of the EN-GJL-150 Cast Iron Matrix Composite with SiC and Al_2O_3 Particles

J. Piątkowski [a, *], M. Wojciechowski [b], J. Fusiarz [a]
[a] Faculty of Materials Engineering, Silesian University of Technology, Poland
[b] Former employee of Brembo. Poland
* Corresponding author: e-mail: jaroslaw.piatkowski@polsl.pl

Received 09.02.26; accepted in revised form 19.03.26; available online 31.08.2026

Abstract

The paper presents an evaluation of the microstructure of a newly developed cast iron–ceramic composite intended for modern braking systems, such as brake discs or brake drums. The composite matrix is grey cast iron with flake graphite (EN-GJL-150), commonly used for brake disc production. The reinforcing phase is a porous ceramic composed of 70 wt.% SiC and 30 wt.% Al_2O_3, intended to enhance the crystallization process and facilitate graphite nucleation in the pearlitic matrix. Microstructural investigations were carried out using digital optical microscopy and scanning electron microscopy (SEM). The results show that reinforcement of the matrix with ceramic particles significantly alters the microstructure of the investigated cast iron. Microstructural analysis of the EN-GJL-150 + SiC + Al_2O_3 composite revealed a previously unreported phenomenon of nucleation occurring at the cast iron–ceramic phase boundary. Consequently, the general assumptions of Riposan's theory concerning the role of oxide micro-inclusions and complex manganese sulphides of the (Mn,X) S type in the nucleation and crystallization of graphite precipitates were confirmed. At the same time, it was found that in the case of *in situ* cast iron–ceramic composites (GJL-150 + SiC + Al_2O_3), this theory should also account for the beneficial role of ceramic particles in promoting a uniform distribution of type A graphite flakes, which nucleate on the surfaces of these particles within the interfacial transition zone. Thus, the nucleation role of oxide micro-inclusions (the first stage of Riposan's theory) could be assumed by SiC and Al_2O_3 particles (Fig. 6), which provide substrates for the heterogeneous nucleation of (Mn, X) S sulphides. The microstructure of such a composite may have a beneficial effect by reducing the wear of friction components in braking systems and decreasing environmental dust emissions from wear products, as required by new European Union regulations, e.g., the EURO 7 standard.

Keywords: EN-GJL-150 cast iron, SiC and Al_2O_3 reinforcing particles, Cast iron microstructure, Graphite nucleation

1. Introduction

Despite increasing quality requirements, traditional grades of cast iron are still widely used in many major industrial sectors, particularly in transport and power engineering [1, 2]. Among these materials, grey cast iron plays an important role due to its numerous advantages, such as the ability to produce castings with complex shapes, good machinability, high vibration damping capacity, and relatively low cost [3-5]. Driven by increasing customer requirements and the need to maintain market competitiveness through high-quality cast iron products, the production process is undergoing continuous development. For these reasons, it is crucial that the graphite formation process is well understood and fully controlled. Graphite nucleation depends on the presence of various substrates in the alloy [6-8], which influence the mechanical

© The Author(s) 2026. Open Access. This article is licensed under a Creative Commons Attribution 4.0 International License (http://creativecommons.org/licenses/by/4.0/), which permits use, sharing, adaptation, distribution and reproduction in any medium or format, as long as you give appropriate credit to the original author(s) and the source, provide a link to the Creative Commons licence, and indicate if changes were made.

properties; these properties can be further improved through heat treatment [9, 10]. Among the main additives in cast irons are those that promote graphite nucleation, such as silicon, manganese, and trace amounts of calcium, aluminium, strontium, barium, and zirconium [11-14]. Their absence or insufficient content causes cast iron to crystallize in a metastable manner, either partially or completely [15, 16]. The role of these additives is to ensure a constant and sufficiently high number of particles that promote graphite formation in the alloy, i.e., so-called heterogeneous nucleation substrates. This ensures stable conditions during the nucleation and growth of graphite flakes, leading to improved service properties of cast iron.

There are many hypotheses concerning graphite nucleation in grey cast irons [17, 18]. One of the best-known is Riposan's theory [19-21]. In simplified form, it assumes a three-stage model of graphite formation:

1. formation of oxides in the alloy (most often with diameters up to ~2 μm), based on strongly deoxidizing elements (e.g., Al, Zr),
2. crystallization of complex sulphides ((Mn,X) S) - usually with sizes up to ~5 μm, which nucleate on the oxides from stage 1,
3. Influence of modifying elements (e.g., Ca, Sr), which enhance the ability of (Mn,X) S sulphides to nucleate graphite due to good crystallographic matching with graphite.

Moreover, the results of studies [19-21] indicate that this model of graphite nucleation requires the addition of strongly deoxidizing elements, such as Al and Zr, into the liquid cast iron, which form a large number of very small micro-inclusions. Additionally, a low sulphur content (up to approximately 0.07 wt.%) is required to allow the crystallization of complex (Mn,X) S-type sulphides, along with residual Al (0.001-0.003 wt.%) [20]. This allows a reduction in the degree of supercooling (ΔT) and the attainment of an appropriate number of eutectic cells in modified cast irons. A lower ΔT promotes the solidification of a favourable eutectic structure with randomly oriented, evenly distributed type A graphite flakes [20].

This theory, although very interesting, does not address the strengthening of the matrix with other additives, such as ceramic particles. According to extensive study results [22], the phenomena occurring during the solidification of cast iron indicate the potential for combining the iron matrix with advanced technical ceramics. The possibility of producing multi-phase materials based on iron is one of the most interesting challenges in modern materials engineering. The interaction between liquid cast iron and ceramic particles, such as aluminium oxide (Al_2O_3) or silicon carbide (SiC), results in a combination of the advantageous physicochemical properties of cast iron and ceramics.

This is mainly related to low wettability, small differences in thermal expansion and thermal conductivity, and a high vibration damping coefficient [22]. Additionally, the formation of nuclei on the ceramic surface is also beneficial, as it strengthens the bonding of the integrated phases in metal matrix composites (MMCs), where the reinforcement, e.g., in the form of particles or fibres, is distributed throughout the matrix to achieve optimal mechanical properties [11].

Therefore, a more detailed understanding of graphite nucleation in grey cast iron containing ceramic particles as a reinforcing phase is crucial. This need arises mainly from the pursuit of improving the performance of cast iron castings used, for example, in braking systems. A controlled microstructure of such castings ensures the production of components capable of absorbing and rapidly dissipating high levels of kinetic energy while meeting stringent environmental standards. It should also be taken into account that non-exhaust emissions, originating mainly from brake and tyre wear, will soon be subject to mandatory limits. The introduction of particulate matter (PM) emission limits imposed by European Parliament regulations under the Euro 7 standard [23] requires a radical change in brake system design. This requirement will apply, among others, to grey cast irons, in which the microstructure will determine the achievement of the required service properties, such as resistance to abrasive wear.

2. Scope and aim of investigations

The aim of the study was to analyse the microstructure of the phase boundary region of a cast-iron composite reinforced with ceramic particles consisting of SiC and Al_2O_3. To achieve the assumed objective, the scope of the study included:

- the development of a concept for melting and casting a GJL-150 grey cast iron composite reinforced with ceramic particles,
- microstructural analysis (LM; SEM),
- proposing a graphite nucleation model for EN-GJL-150 cast iron reinforced with ceramic particles

3. Research materials and methodology

Commercial EN-GJL-150 cast iron, used for the production of brake discs and brake drums, was selected for the study. The cast iron, modified with the Elkem SuperSeed inoculant (0.15-0.25%), was poured at a temperature range of 1430–1450 °C into a sand mould with dimensions of 300 × 300 mm and a mould cavity measuring 150 × 100 × 20 mm. In the central part of the moulding box, a porous insert was placed, characterized by an open porosity of 10 ppi (pores per inch). Its purpose was to enable the formation of a cast iron-ceramic particle composite. The proportion of reinforcing particles (70 wt.% SiC and 30 wt.% Al_2O_3) was selected based on industrial practice [24] and previous studies [25]. The technology for producing cast iron-ceramic composites, in which the reinforcing phase is a ceramic foam made of SiC and Al_2O_3 with an activated surface, was presented in studies [26].

Light microscopy (LM) microstructural studies were conducted using a Leica MEF-4M optical microscope (Leica Microsystems GmbH, Wetzlar, Germany) and a VHX-X1 digital microscope (Keyence International, Mechelen, Belgium). SEM studies were carried out using a Tescan MIRA scanning electron microscope (Tescan Brno, Brno, Czech Republic). The investigations were performed on polished and etched metallographic specimens, using nital and Stead's reagent.

Ten micrographs were taken, from which representative images of the microstructure of the investigated cast iron with ceramic particles were selected. The schematic diagram and the sampling location are shown in Figure 1.

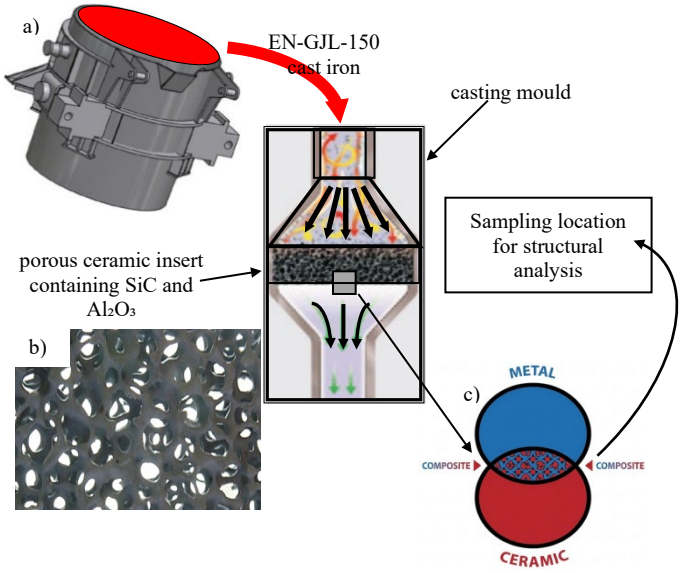


Fig. 1. Schematic of the cast iron pouring process (a) into a mould containing a porous insert with ceramic particles (b), and the location of samples cut for microstructural analysis (c)

The choice of SiC and Al_2O_3 is based on their very high hardness (2200–2800 HV) and thermal conductivity: 320-490 $W \cdot (m \cdot K)^{-1}$ for SiC. However, the main reason for selecting these particles as reinforcement is their chemical activity with cast iron.
The reactivity of SiC at casting temperatures (approximately 1430-1450 °C) promotes wetting by the cast iron, since the contact angle of SiC decreases below 90° at temperatures up to about 1600 °C, where SiC diffusion into cast iron becomes very intense. In addition, silicon is a strongly graphitizing element, which increases the thermodynamic activity of carbon in the liquid solution and reduces its solubility. This leads to local supersaturation of the melt with carbon, which, being unable to remain in solution, precipitates as numerous small graphite nuclei that remain active for a long time after introduction into the melt. On the other hand, the advantage of Al_2O_3 is its high mechanical and thermal stability. Once incorporated into the composite, it serves as an architectural, stable structural skeleton for the porous insert, resistant to geometrical changes during solidification.

4. Results

The chemical composition of the cast iron is presented in Table 1. Representative microstructures of the EN-GJL-150 composite with SiC and Al_2O_3 particles are shown in Figs. 2-6.

Table 1.
Chemical composition of EN-GJL-150 cast iron

Elemental content, wt.%*						
C	Si	Mn	P	S	Fe	others*
3.5-3.8	1.5-1.7	0.6-0.8	<0.2	0.06-0.09	93.0-94.0	Al.; Sr; Zr

* - up to approx. 0.005 wt.% Al; up to 0.008 wt.% Sr; up to 0.006 wt.% Zr. These are the elements contained in the Elkem SuperSeed inoculant.

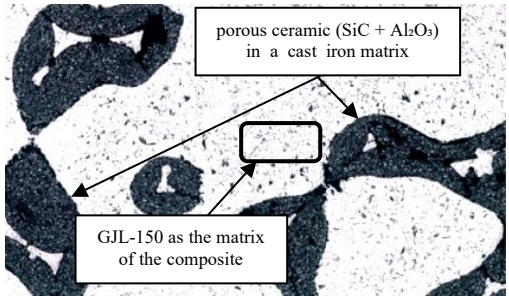


Fig. 2. Representative LM microstructure of the cast iron composite reinforced with ceramic particles – unetched sample

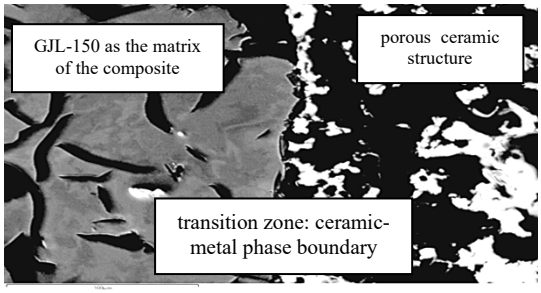
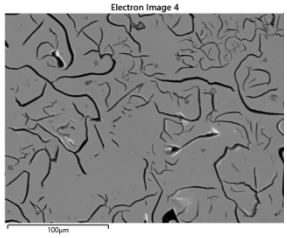


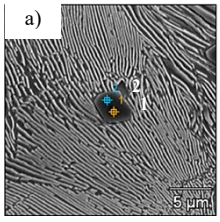
Fig. 3. SEM microstructure of the cast iron–porous ceramic interface



Graphite type*	A 75%	E 15%	B 10%
Graphite morphology	Flake		
Size*	3	4	5
Matrix	100% pearlite		

* - Based on the standard PN-EN ISO 945-1: Microstructure of cast irons – Part 1: Classification of graphite precipitates by visual analysis.

Fig. 4. SEM microstructure of the EN-GJL-150 and quantitative analysis of graphite precipitation



b)

wt.%	O	Mg	Al	Si	S	Mn
Point 1	20.0	1.4	18.5	2.3	20.6	37.3
Point 2	---	---	0.3	---	31.3	68.8
at.%						
Point 1	38.8	1.7	20.2	2.4	19.0	20.0
Point 2	---	---	0.4	---	43.4	56.2

Fig. 5. SEM microstructure of the EN-GJL-150 + SiC + Al_2O_3 (a) composite and the results of chemical composition microanalysis (b)

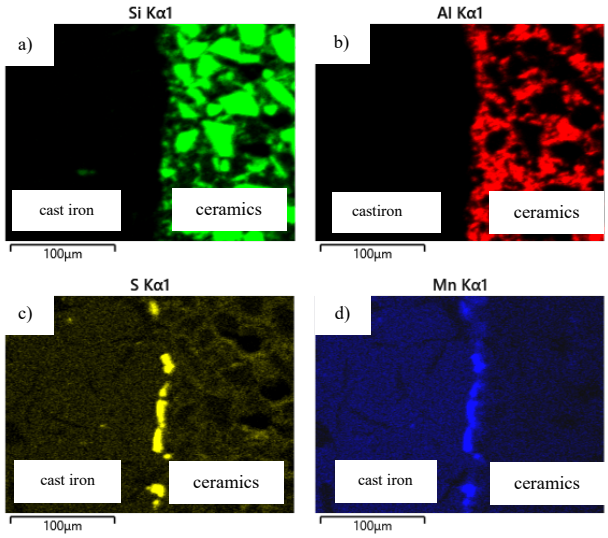


Fig. 6. Maps of the relative elemental concentration at the cast iron–ceramic phase boundary: a) silicon carbide – component of the porous ceramic (70% SiC); b) 30% Al_2O_3; c) sulphur; d) manganese present in (Mn,X) S

5. Discussion of results

Quantitative tests of the microstructure of the developed composites were performed in accordance with the PN-EN ISO 945-1 standard. Microstructure of cast iron - Part 1 Classification of graphite precipitations based on visual analysis (Fig. 4). The size of graphite flakes ranges from 3 to 5. There is no degeneration of graphite precipitates and no presence of cementite in the transition zone. Due to technical difficulties in digestion, quantitative measurements of eutectic cells were not performed. In the cast iron region, type A graphite precipitates are still present and are uniformly distributed within the iron matrix. However, it should be emphasized that studies on the influence of SiC and Al_2O_3 particles on changes in the morphology of EN-GJL-150 cast iron microstructural constituents should be continued and are currently at the stage of further experimental investigations.

A particular advantage of grey cast iron is the low cost of its castings. This also applies to the addition of porous ceramics, in contrast to carbide powder additives, which are more expensive. This can be achieved in various ways [6-9]; however, an innovative approach to reinforcing the iron matrix is the introduction of ceramic particles, such as SiC and Al_2O_3, as used in this study.
Such a combination of the matrix and reinforcing phase allows for enhanced mechanical and tribological properties, as well as improved heat dissipation (thermal conductivity of cast iron $\lambda = 48$-60 $W \cdot m^{-1} \cdot K^{-1}$, whereas for SiC it is approx. 120-360 $W \cdot m^{-1} \cdot K^{-1}$, while maintaining costs at a level comparable to traditional cast iron melting and modification methods.

The present study focuses on the microstructural analysis of the developed EN-GJL-150 + SiC + Al_2O_3 composite.

The reinforcement used in this study is a porous structure of the "ceramic foam" type, with a pore density of 10 PPI (pores per inch), corresponding to a structure with large, open cells that facilitate the free flow of molten metal, minimizing hydraulic resistance during the filling of the ceramic insert. The reinforcement, with a chemical composition of 70 wt.% SiC and 30 wt.% Al_2O_3, determines a series of complex reactions at the metal-ceramic phase boundary. It should be emphasized that the introduction of a foreign ceramic foam phase into cast iron significantly alters the crystallization conditions. The method of composite fabrication presented in this study leads to the combination of bulk crystallization (on endogenic inclusions) and surface crystallization (on the exogenous reinforcement). This results in the formation of a unique microstructure in the transition zone (Fig. 3).

The EDS test results confirm the presence of manganese and sulfur in the interfacial area, but this zone is not continuous along the entire length of the connection. Its thickness (from approx. 40 to 80 µm) depends on the diffusion zone of SiC grains. The positive effect on the change in the morphology of graphite flakes is due to the local supersaturation of the cast iron matrix with carbon and silicon according to the reaction:

$$SiC + Fe \rightarrow FeSi + C, \quad (1)$$

which play a catalytic role in the graphite nucleation process.
Aluminium oxide, a passive and stabilizing component, ensures the mechanical integrity of the porous structure (ceramic framework) at high temperatures. It is a material with high bonding energy and relatively poor wettability by liquid cast iron (contact angle $\theta > 90°$ in non-reactive systems). Its role is to form a stable reinforcing system, typical of a composite.

Silicon carbide acts as an active (reactive) component. At the casting temperatures of grey cast iron (1430-1450 °C), SiC is thermodynamically unstable in contact with an iron-silicon alloy and decomposes according to the reaction [22]:

$$SiC_{(S)} + Fe_{(L)} \rightarrow FeSi_{(L)} + C_{(g)} \quad (2)$$

where:
S – liquid state; L – liquid state, g – graphite.

Reaction (2) is crucial for the formation of microstructural constituents. The release of silicon and carbon atoms into the iron–ceramic transition zone (Fig. 3) causes strong local supersaturation with these elements.

Silicon, a strongly graphitizing element, increases the thermodynamic activity of carbon, promoting its precipitation as graphite. SiC thus acts as an "in situ" modifier. This is a desirable phenomenon that prevents the formation of hard and brittle iron carbides (cementite) in the interface zone.

In the studied composite system, Riposan's theory [19-21] must be extended to include the influence of a macroscopic substrate in the form of a porous structure. This structure causes an uneven crystallization front, with its geometry governed by SiC surface diffusion.
Nucleation on concave surfaces (pockets, cracks in the ceramic reinforcement) is energetically favoured. The porous structure, full of microcracks and depressions on the surface of the sintered SiC + Al_2O_3 particles, acts as a "geometric catalyst" for crystallization, promoting nucleation even under conditions where chemical wettability is insufficient. A schematic illustration of graphite nucleation is shown in Figure 7.

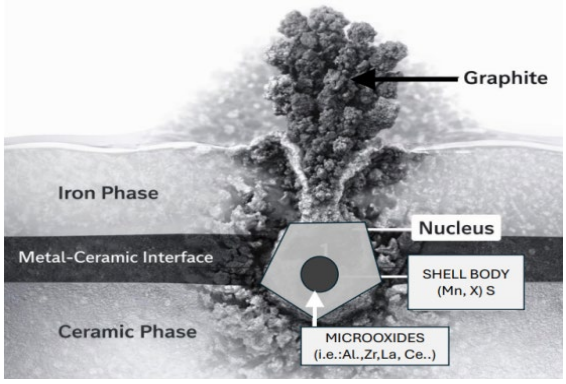


Fig. 7. Schematic illustration of graphite nucleation at the cast iron–ceramic phase boundary in the EN-GJL-150 + SiC + Al_2O_3 composite

The proposed modification of Riposan's theory therefore assumes coexistence of two graphite flake nucleation processes (Fig. 8):

1. In accordance with Riposan's model, deep within the metallic matrix and away from the ceramic walls, graphite nucleates on (Mn,X) S-type sulphides, which in turn grow on $(Al,Mg)_XO_Y$ oxide microinclusions. This is confirmed by the presence of MnS inclusions.
2. Surface-assisted nucleation (transition zone nucleation). At the phase boundary, the reinforcement surface-rich in oxides and carbides and characterized by a highly developed topography-assumes the role of the oxide microinclusions from the first stage.(Mn,X) S-type sulphides readily nucleate on the rough ceramic surface, forming an intermediate layer on which graphite grows directionally. This explains the very good adhesion of graphite to the ceramic phase and the absence of a graphite-free zone.

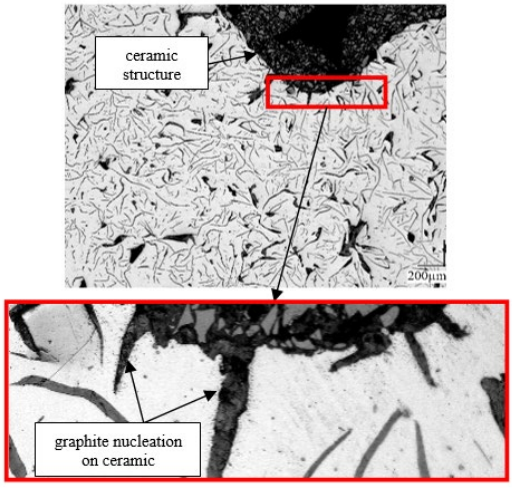


Fig. 8. Microstructure of the EN-GJL-150 + SiC + Al_2O_3 composite showing graphite flakes nucleating on the ceramic particles and on (Mn,X) S-type sulphides

It should be noted that studies on the influence of SiC and Al_2O_3 particles on changes in the morphology of the microstructural constituents of EN-GJL-150 cast iron, particularly with regard to graphite nucleation, should be continued and are currently at the stage of further experimental investigations.

It is also worth noting that the presented concept of obtaining composites using a porous structure containing ceramic SiC and Al_2O_3 particles shows significant research potential in the field of joining cast iron with ceramics. At this stage of the research, the material appears to meet the required functional properties; however, further studies should be conducted to assess its influence on other material characteristics, such as strength, fatigue resistance, heat dissipation, thermal shock resistance, etc.

6. Conclusions

The results of the present study allow the following conclusions to be drawn:

1. The "foam" structure consisting SiC and Al_2O_3 particles acts as an active catalyst for graphite crystallization. As a result, unfavourable cementite precipitates in the transition zone can be eliminated, which has previously been a problem in similar material systems. This structural integrity at the cast iron–ceramic phase boundary is a direct result of favourable crystallographic matching between the ceramic phase and the newly formed metallic phases.
2. SEM images reveal a distinct phase boundary between the cast iron and the porous ceramic structure. Importantly, no cracks, delaminations, or gas porosity commonly observed in situ cast composites were detected. This confirms the correct selection of pouring parameters and adequate wettability of the ceramic by the liquid metal. It is worth noting that at a SiC content of 70 wt.%, the ceramic phase is reactive, which promotes chemical wetting.
3. Analysis of the morphology of graphite and the matrix in the transition zone, as well as in the conventional matrix, reveals the presence of a fully pearlitic structure. No fragmented or degenerated graphite was observed, which is a common issue when cast iron comes into contact with a foreign reinforcing phase. In contrast, type A flake graphite with a homogeneous distribution is visible.
4. Intensive graphite growth on the ceramic was observed. Graphite flakes "growing" on the ceramic surface are clearly visible (Fig. 8). This suggests that the reinforcement surface has assumed the role of a heterogeneous nucleation site.
5. It can be stated that the reaction of cast iron with SiC locally created a region rich in carbon and silicon, which significantly increases the potential for graphitization. Manganese and sulphur contained in the (Mn,X) S sulphides at the cast iron–ceramic phase boundary represent the main modification validating Riposan's model.
6. A significant correlation was observed between the presence of manganese and sulphur in the transition zone. This suggests that the ceramic surface may have acted as a substrate for the nucleation of sulphides (replacing the oxide microinclusions from the first stage of the nucleation process), which in turn initiated graphite growth. This provides evidence of the synergistic action of endogenic and exogenic nucleation processes.

References

[1] Praveen Babu, R. & Praveen, K. (2013). Machinability studies of peripheral milling on pearlitic cast iron. *Advanced Materials Research.* 685, 86-91, https://doi.org/10.4028/www.scientific.net/AMR.685.86.

[2] Stefanescu, D.M., Suarez, R. & Kim, S.B. (2020). 90 years of thermal analysis as a control tool in the melting of cast iron. *China Foundry.* 17(2), 69-84. https://doi.org/10.1007/s41230-020-0039-x.

[3] Malakizadi, A. & Nyborg, L. (2023). Machining of bi-metallic aluminium-grey cast iron engine block - process optimisation by means of FEM. *Procedia CIRP*. 117, 323-328. https://doi.org/10.1016/j.procir.2023.03.055.

[4] Mitelea, I., Bordeaşu, I., Riemschneider, E., Uţu, D. & Craciunescu, C. (2022). Cavitation erosion improvement following TIG surface-remelting of gray cast iron. *Wear.* 496-497, 204282, 1-10. https://doi.org/10.1016/j.wear.2022.204282.

[5] Gu, J., Luo, C., Zhang, P., Ma, P. & Ren, X. (2020). Laser cavitation peening of gray cast iron: Effect of coverage layer on the surface integrity. *Applied Surface Science*. 521, 146295, 1-9. DOI: 10.1016/j.apsusc.2020.146295.

[6] Upadhyay, S. & Saxena, K.K. (2020). Effect of Cu and Mo addition on mechanical properties and microstructure of grey cast iron: An overview. *Materials Today: Proceedings.* 26, 2462-2470. https://doi.org/10.1016/j.matpr.2020.02.524.

[7] Darmawan, A.S., Anggono, A.D., Yuliant, O.A., Febriantoko, B.W. & Masyrukan, Hamid A. (2022). Comparison of microstructure, yield strength, tensile strength, and modulus of elasticity between gray cast iron and nodular cast iron. *Key Engineering Materials*. 935, 25-32. https://doi.org/10.4028/p-2094w8.

[8] Darmawan, A.S., Yulianto, A., Febriantoko, B.W., Masyrukan, Ginta T.L. & Hamid, A. (2023). Engineering hardness and toughness of gray cast iron with the addition of silicon elements. *Journal of Physics*. *Conference Series.* 2972, 012042, 1-9. https://doi.org/10.1088/1742-6596/2972/1/012042.

[9] Hariningsih, H., Lutiyatmi, L. & Daryanto, T. (2022). Effects of heat treatment on microstructure and hardness of D2 tools. *Applied Research and Smart Technology.* 3(1), 31-40. https://doi.org/10.23917/arstech.v3i1.761.

[10] Sugito, B., Anggono, A.D. & Qomarudin, A. (2020). Influence of annealing and normalizing treatment to the hardness and microstructure of friction stir welding Al-5052. *Journal of Emerging Trends in Engineering Research.* 8(9), 5362-5366.

[11] Guzik, E., Kopyciński, D., Ziółko, A. & Szczęsny, A. (2023). The method of inoculation of high-quality grey cast iron intended for massive castings for bottom and distance plates as well counterweights manufactured as vertical castings. *Archives of Metallurgy and Materials*. 68(1), 359-368. https://doi.org/10.24425/amm.2023.141512.

[12] Yakut R. (2023). Investigation of mechanical properties of grey cast irons reinforced with carbon titanium nitride (TiNC). *Lubricants*. 11(10), 454, 1-12. https://doi.org/10.3390/lubricants11100454.

[13] Sommerfeld, A. & Tonn, B. (2009). Theory of graphite nucleation in lamellar graphite cast iron. *International Journal of Metalcasting.* 3(4), 39-47, https://doi.org/10.1007/BF03355457.

[14] Riposan, I. (2010). Role of lanthanum in graphite nucleation in grey cast iron. *Key Engineering Materials.* 457, 19-24, https://doi.org/10.4028/www.scientific.net/KEM.457.19.

[15] Leube, B. (1996). *Contribution to the modeling of the cooling and crystallization of eutectic cast iron alloys with lamellar graphite.* PhD Thesis, TU Bergakademie Freiberg, Freiberg, Germany.

[16] Basdogan, M.F., Bennett, G.H.J., Kondic, V. (1980). Effects of sulphur and oxygen on solidification of grey cast iron. *Solidification Technology in the Foundry and Cast House, Proceedings, The Metals Society, Conventry*. 240-247.

[17] Alonso, G., Stefanescu, D.M., Larranaga, P. & Suarez, R. (2020). Graphite nucleation in compacted graphite cast iron. *International Journal of Metalcasting.* 14(2), 1162-1171. https://doi.org/10.1007/s40962-020-00441-2.

[18] Gorka, A.M. (2019). *Nucleation and growth of graphite in cast iron*. PhD Thesis, Transilvania Universita of Brasov, Faculty of Materials Science and Engineering.

[19] Riposan, I., Chisamera, M., Stan, S., Hartung, C. & White, D. (2010). Three-stage model for nucleation of graphite in grey cast iron. *Materials Science and Technology*. 26(12), 1439-1447. https://doi.org/10.1179/026708309X12495548508626.

[20] Chisamera, M., Riposan, I., Stan, S., White, D. & Grasmo, G. (2008). Graphite nucleation control in grey cast iron. *International Journal of Cast Metals Research*. 21(1-4), 39-44. https://doi.org/10.1179/136404608X361639.

[21] Riposan, I., Chisamera, M. & Stan, S. (2013). Enhanced quality in electric melt grey cast irons. *ISIJ International*. 53(10), 1683-1695. https://doi.org/10.2355/isijinternational.53.1683.

[22] Chawla, K.K. (2019). *Composite Materials: Science and Engineering* (4th ed.). New York, USA: Springer.

[23] Regulation (EU) No 2024/1257 of the European Parliament and of the Council of 24 April 2024 – PE/109/2023/REV/2, http://data.europa.eu/eli/reg/2024/1257/oj.

[24] Röhrle, M.D. (1995). *Pistons for internal combustion engines: Fundamentals of piston technology*. Landsberg/Lech, Germany: Verlag Moderne Industrie.

[25] Posmyk A. & Myalski J. (2017). Composites including foam inserts designed for combustion engines cylinder liners. *Composites, Theory and Practice*. 17(1), 25-29.

[26] Posmyk, A. & Myalski, J. (2022). Composite material with cast iron matrix designed for brake systems of technical means of transport. *Tribologia*. 301(3), 79-86, https://doi.org/10.5604/01.3001.0016.1036.